Overproduction of the N-terminal Anticodon-binding Domain of the Non-discriminating Aspartyl-tRNA Synthetase from Helicobacter pylori for Crystallization and NMR Measurements.

ARTICLE *in* PROTEIN EXPRESSION AND PURIFICATION · FEBRUARY 2013

Impact Factor: 1.7 · DOI: 10.1016/j.pep.2013.02.006 · Source: PubMed

Protein Expression and Purification 89 (2013) 25–32

Contents lists available at SciVerse ScienceDirect

Protein Expression and Purification

journal homepage: www.elsevier.com/locate/yprep

Overproduction of the N-terminal anticodon-binding domain of the non-discriminating aspartyl-tRNA synthetase from *Helicobacter pylori* for crystallization and NMR measurements

Pitchayada Fuengfuloy [a], Pitak Chuawong [a,*], Suwimon Suebka [a], Pakorn Wattana-amorn [a], Christopher Williams [b], Matthew P. Crump [b], Chomphunuch Songsiriritthigul [c]

[a] Department of Chemistry and Center of Excellence for Innovation in Chemistry, Faculty of Science, Kasetsart University, 50 Ngamwongwan Rd., Chatuchak, Bangkok 10900, Thailand
[b] School of Chemistry, University of Bristol, Cantock's Close, Clifton, Bristol BS8 1TS, UK
[c] Synchrotron Light Research Institute (Public Organization), 111 University Avenue, Nakhon Ratchasima, Thailand

ARTICLE INFO

Article history:
Received 5 December 2012
and in revised form 6 February 2013
Available online 27 February 2013

Keywords:
Non-discriminating aspartyl-tRNA synthetase
Anticodon-binding domain
Helicobacter pylori
Protein NMR
X-ray crystallography

ABSTRACT

Aminoacyl-tRNA synthetases (aaRSs) covalently attach an amino acid to its cognate tRNA isoacceptors through an ester bond. The standard set of 20 amino acids implies 20 aaRSs for each pair of amino acid/tRNA isoacceptors. However, the genomes of all archaea and some bacteria do not encode for a complete set of 20 aaRSs. For the human pathogenic bacterium *Helicobacter pylori*, a gene encoding asparaginyl-tRNA synthetase (AsnRS) is absent whilst an aspartyl-tRNA synthetase (AspRS) aminoacylates both $tRNA^{Asp}$ and $tRNA^{Asn}$ with aspartate. The structural and functional basis for this non-discriminatory behavior is not well understood. Here we report the over-production of the N-terminal anticodon-binding domain of *H. pylori* ND-AspRS using *Escherichia coli* BL21(DE3) host cells. Prolonged expression of this protein resulted in a toxic phenotype, limiting the expression period to just 30 min. Purified protein was monomeric in solution by gel filtration chromatography and stable up to 42 °C as observed in temperature-dependent dynamic light scattering measurements. Circular dichroism indicated a mixture of α-helix and β-sheet secondary structure at 20 °C and predominantly β-sheet at 70 °C. Optimized crystallization conditions at pH 5.6 with PEG 4000 as a co-precipitant produced well-formed crystals and ^{1}H NMR spectrum showed a well dispersed chemical shift envelope characteristic of a folded protein.

Introduction

Aminoacylation of tRNA is a crucial process for all forms of life on earth. The fidelity of ribosomal protein biosynthesis strongly depends on the generation of correctly aminoacylated tRNAs [1–3]. The enzymes that govern this important cellular process are aminoacyl-tRNA synthetases (aaRSs)[1]. Since all known organisms utilize the 20 standard amino acids for ribosomal protein synthesis, one would expect the existence of 20 aaRSs, one for each pair of amino acid/tRNA isoacceptors. In all archaea and some bacteria, however, the rule of one aaRS per amino acid/tRNA isoacceptors pair does not apply. These organisms lack gene(s) encoding certain aaRS(s), and unavoidably rely on an indirect aminoacylation process to produce a full set of correctly aminoacylated tRNAs [1–4]. The frequently missing aaRSs are glutaminyl-tRNA synthetase (GlnRS) and/or asparaginyl-tRNA synthetase (AsnRS). In the absence of GlnRS and/or AsnRS, a two step indirect aminoacylation takes place. First, the incorrectly aminoacylated Glu-$tRNA^{Gln}$ and/or Asp-$tRNA^{Asn}$ are generated via the activity of the non-discriminating GluRS [5–16] or, in some cases, GluRS2 [10,11,17–21] and/or a non-discriminating AspRS (or AspRS2) [12,22–35]. In bacteria, these misacylated tRNAs are subsequently converted to correctly aminoacylated Gln-$tRNA^{Gln}$ and/or Asn-$tRNA^{Asn}$ by the heterotrimeric glutamine-dependent Asp-$tRNA^{Asn}$/Glu-$tRNA^{Gln}$ amidotransferase (GatCAB) [13,27,36–38].

Due to the lack of genes encoding GlnRS and AsnRS, the human pathogen *Helicobacter pylori* relies on an indirect pathway for the biosynthesis of Gln-$tRNA^{Gln}$ and Asn-$tRNA^{Asn}$ [39]. In this case, GluRS2 [21] and the non-discriminating AspRS (ND-AspRS) [24]

* Corresponding author. Fax: +66 2 5625555x5161.
E-mail address: Pitak.C@ku.ac.th (P. Chuawong).

[1] Abbreviations used: aaRS, aminoacyl-tRNA synthetase; GluRS, glutamyl-tRNA synthetase; GluRS2, glutamyl-tRNA synthetase 2; GlnRS, glutaminyl-tRNA synthetase; AspRS, aspartyl-tRNA synthetase; ND-AspRS, non-discriminating aspartyl-tRNA synthetase; ND-$AspRS_{1-104}$, the N-terminal anticodon-binding domain of the non-discriminating aspartyl-tRNA synthetase; GatCAB, Asp-$tRNA^{Asn}$/Glu-$tRNA^{Gln}$ amidotransferase; WT, wild-type; *H. pylori, Helicobacter pylori; E. coli, Escherichia coli; P. aeruginosa, Pseudomonas aeruginosa; P. falciparum, Plasmodium falciparum; B. stearothermophilus, Bacillus stearothermophilus*; OD_{600}, optical density at 600 nm; LB, Luria–Bertani; IPTG, isopropyl-β-D-1-thiogalactopyranoside; Ni-NTA, nickel-nitrilotriacetic acid; DLS, dynamic light scattering; CD, circular dichroism; EDTA, ethylenediaminetetraacetic acid; PEG 4000, polyethylene glycol with average molecular weight of 4,000 g/mol; NMR, nuclear magnetic resonance; DPFGSE, double pulsed field gradient spin-echo; ppm, parts per million

1046-5928/$ - see front matter © 2013 Elsevier Inc. All rights reserved.
http://dx.doi.org/10.1016/j.pep.2013.02.006

are responsible for the generation of incorrectly aminoacylated Glu-tRNA^{Gln} and Asp-tRNA^{Asn}. These erroneously aminoacylated tRNA species are converted to correctly aminoacylated Gln-tRNA^{Gln} and Asn-tRNA^{Asn} by the GatCAB [24,40,41], hence the fidelity of ribosomal protein biosynthesis in *H. pylori* is ensured.

While *H. pylori* GluRS2 only generates misacylated Glu-tRNA^{Gln} [21], the ND-AspRS exhibits dual tRNA specificity, and aminoacylates both tRNA^{Asp} and tRNA^{Asn} with aspartate [24]. The relaxed tRNA specificity in bacterial type ND-AspRS, such as the one from *H. pylori*, is not well understood, despite several related crystal structures. All of the ND-AspRS structures reported to date [30,42,43], including the transamidosome transfer-ribonucleoprotein [44], are archaeal in origin. Mutations in the anticodon binding domain of the bacterial-type ND-AspRS from *Pseudomonas aeruginosa* (H31L and G83K) [25] and *H. pylori* (L81N and L86M) [24] have been analyzed. The mutations in *H. pylori* ND-AspRS increased *H. pylori* tRNA^{Asp} specificity, whereas *P. aeruginosa* mutants did not show significant impact in tRNA specificity when tested against it's native tRNAs. Apparently, the role of these previously reported anticodon-binding domain mutations in tRNA recognition are not fully understood. Consequently, obtaining structural information of the anticodon-binding domain from solution NMR and crystal structures will help to unravel the peculiar tRNA specificity of the bacterial-type ND-AspRS.

We have reported herein the cloning, overexpression, and purification of ND-AspRS$_{1\text{-}104}$ (the N-terminal anticodon-binding domain of the ND-AspRS) from *H. pylori*. The protein is stable and exists as a monomer in solution. The heterologous overexpression of this protein in *E. coli* exhibits a toxic phenotype which has also been observed when the full length wild-type ND-AspRS from *H. pylori* was overexpressed in *E. coli* [24]. The NMR and CD spectroscopic results indicate a properly folded protein comprised of both β-sheet and α-helix secondary structure. The NMR and crystallization conditions have been optimized and this preliminary work will enable both NMR and crystal structure elucidations for this protein.

Material and methods

Bacterial strains, plasmids, media, and chemicals

Vector amplification and cloning experiments were conducted using *E. coli* strain DH5α. Overexpression of the recombinant proteins was accomplished using the BL21(DE3) strain of *E. coli*. The pCDF-1b expression vector (Novagen) was used in the construction of expression vector pPC010. Host cells were grown in LB (Luria Bertani) medium containing 1% tryptone, 0.5% yeast extract, and 1% sodium chloride supplied with streptomycin to a final concentration of 50 μg/mL. Unless stated otherwise, all chemicals were purchased from Fluka and Amersham Biosciences (Currently GE Healthcare Life Sciences). Restriction endonucleases were obtained from Fermentas. Plasmids were purified using the High-Speed Plasmid Mini Kit from Geneaid Biotech Ltd. Affinity chromatography was performed using Ni-NTA Spin Columns from Qiagen. Vivaspin™ sample concentrators were purchased from GE Healthcare Life Sciences. DNA sequencing was performed by MACROGEN (Macrogen Inc., Seoul, South Korea).

Cloning of the H. pylori ND-AspRS$_{1\text{-}104}$

The gene encoding the *H. pylori* ND-AspRS$_{1\text{-}104}$ was amplified from pPTC001 [24], the plasmid encoding the wild-type ND-AspRS from *H. pylori*. The forward primer PtDS03 (5′-CGGGGTACCATGCGAAGTCATTTTTGC-3′) and reverse primer PtDS04 (5′-CCAATGCATTGGTTCTGCAGTTAGCTTTTATTTTC-3′) allowed the introduction of flanking *KpnI* and *PstI* restriction sites to facilitate cloning into the pCDF-1b vector and incorporation of an N-terminal six histidine affinity tag. The ligated product (pPC010) was introduced into chemically competent *E. coli* DH5α cells and positive transformants were selected on LB agar plates containing 50 μg/mL streptomycin. The identity of the construct was confirmed by DNA sequencing of the entire open reading frame.

Growth studies

Cell viability profiles of *E. coli* strain BL21(DE3) overexpressing the *H. pylori* ND-AspRS$_{1\text{-}104}$ and the full length wild-type *H. pylori* ND-AspRS were evaluated. In each case, the experiment started by growing a 5 mL overnight culture of a single colony picked from an agar plate supplied with streptomycin. The temperature was maintained at 37 °C and the culture was continuously agitated. The overnight culture was then used to inoculate 200 mL culture of the same medium at 37 °C with agitation to an OD_{600} of 0.05. Protein expression was induced by addition of isopropyl-β-D-1-thiogalactopyranoside (IPTG) to a final concentration of 1 mM. Growth was monitored over 8.8 h. No expression control for each protein was conducted using cultures supplied with 50 μg/mL streptomycin and 0.5% glucose. The data reported herein represents the average from experiments conducted in triplicate.

Overexpression and purification of the H. pylori ND-AspRS$_{1\text{-}104}$

Chemically competent expression host cells, *E. coli* BL21(DE3), were transformed with pPC010 via heat-shock procedure. Positive transformants were selected on an LB-agar plate supplemented with streptomycin, inoculated in a 5 mL LB medium containing streptomycin and grown overnight at 37 °C with agitation. The starter overnight cell culture was diluted into 300 mL LB medium supplemented with streptomycin, and grown at 37 °C with agitation. Once the OD_{600} had reached 0.8, the expression of the protein was induced via the addition of IPTG to a final concentration of 1 mM. The cell culture was induced for 30 min. Subsequently, the cells were harvested through centrifugation at 4,000 rpm for 15 min at 4 °C. Protein purification was conducted according to the manufacturer's instructions with a slight modification during the wash step. Briefly, the Ni-NTA bound protein was washed with 15 mM, 20 mM, and 30 mM gradient concentrations of imidazole. The protein was eluted with elution buffer containing 250 mM imidazole, 50 mM sodium dihydrogenphosphate, and 300 mM sodium chloride at pH 8.0. The eluted protein fraction was subjected to a series of buffer exchange steps with 10 mM phosphate buffer pH 7.0 using Vivaspin™ (10 kDa molecular weight cutoff) in order to remove imidazole. The proteins were kept in storage buffer containing 50% glycerol, 33 mM phosphate buffer at pH 7.4, 2 mM Tris-Cl, 1.5 μM β-mercaptoethanol, and 0.5 mM phenylmethanesulfonyl fluoride as a protease inhibitor. The protein was further purified by gel filtration (Hiprep 16/60 Sephacryl S-200 HR column, 120 mL) in 50 mM phosphate buffer with 150 mM sodium chloride at pH 8.0. The flow rate used in all experiments was 0.5 mL/min, and the column was calibrated using a low molecular weight gel filtration calibration kit (GE Healthcare Life Sciences). The purified protein was analyzed using 8% sodium docecyl sulfate-polyacrylamide gel electrophoresis (SDS–PAGE). Protein concentration was determined by BCA protein assay (Pierce) using BSA as a standard protein.

Western blot analysis

The six histidine tagged ND-AspRS$_{1\text{-}104}$ of *H. pylori* was analyzed by western blot using Trans-Blot® SD (BIO-RAD). The protein was transferred to a BioTrace™ PVDF membrane (PALL Life Sciences)

and detected using the SuperSignal® West HisProbe™ Kit (Thermo Scientific). The protein band was visualized on a Fusion FX7 image acquisition system (Vilber Lourmat, France).

Dynamic light scattering

DLS analyses were performed on a Zetasizer Nano series (Nano-ZS zen 3600, Malvern Instruments Ltd, UK) using standard operating procedures (SOP) for temperature trend measurements. The 16 μM solution of the *H. pylori* ND-AspRS$_{1\text{-}104}$ in 100 mM phosphate buffer at pH 7.5 containing 50 mM KCl, 0.1 mM EDTA, 10 mM β-mercaptoethanol was introduced into a ZEN0040 disposable micro cuvette. The temperature interval was 1.0 °C with an equilibration time of 120 s. The experiment was conducted from 20–50 °C. Corrections for solvent refractive index and viscosity were applied and the data were processed using multiple narrow modes. The average particle size (Z-Ave) was reported in nanometers as a function of temperature.

Circular dichroism spectroscopy

CD spectra were recorded on J-815 circular dichroism spectropolarimeter (Jasco, UK) using a 90 μM protein solution (10 mM phosphate, pH 7.0) in a 1 mm path length cuvette. The sample was scanned in the range of 190 to 260 nm and 10–80 °C in 10 °C intervals. The sample was then cooled down to 60, 40, and 20 °C where the CD spectra were recorded again. The CD spectrum at 20 °C was subjected to the secondary structure content analysis using three different algorithms in CDPro program; SELCON3, CDSTR, and CONTINLL [45]. The percentage of α-helix and β-sheet was averaged from these three algorithms.

1D ^{1}H NMR spectroscopy

The NMR sample was prepared by dissolving the *H. pylori* ND-AspRS$_{1\text{-}104}$ in 50 mM phosphate buffer, 150 mM sodium chloride at pH 8.0, and 8% deuterated water (D_2O) to a final concentration of 250 μM. A standard one-dimensional double pulsed field gradient spin-echo (DPFGSE) [46] was acquired at 25 °C on a 600 MHz Varian VNMRS cryo-probe equipped spectrometer.

X-ray crystallography

Crystal screens (JBScreen Classic HTS I, Jena Bioscience, Germany) of the *H. pylori* ND-AspRS$_{1\text{-}104}$ were initiated (7.75 mg/mL, 18 °C). The crystallization was observed in 30% (w/v) PEG 4000, 100 mM ammonium sulfate, 100 mM sodium citrate at pH 5.6. Blank conditions were set up in order to confirm that the morphology observed was the result of protein crystallization. Subsequently, crystallization conditions with PEG 4000, ammonium sulfate, and sodium citrate were optimized using hanging drop trays.

Results and discussions

Cloning, overexpression, purification, and Western blot analysis of the H. pylori ND-AspRS$_{1\text{-}104}$

In the absence of a crystal structure for a bacterial type ND-AspRS, cloning primers that spanned the entire anticodon-binding domain gene were designed based on a homology model of *H. pylori* ND-AspRS. This model was constructed using the Geno3D server [47] with *E. coli* AspRS (PDB ID: 1C0A) as a template. The model indicated Asn102 was likely to be the terminal amino acid located in the β-barrel of the domain and primers were constructed that covered Met1-Ser104 (Fig. 1A). The cDNA was inserted into the pCDF-1b vector to yield pPC010 and a 115 amino acid construct including the N-terminal 6His-tag (Fig. 1B). The *E. coli* BL21(DE3) host cells transformed with pPC010 were grown to late log phase, and expression was induced with IPTG. Although the overexpression of full-length ND-AspRS from *H. pylori* is toxic to *E. coli* host cells due to the generation of incorrectly charged Asp-tRNA^{Asn} by *H. pylori* ND-AspRS using *E. coli* tRNA^{Asn} [24], we did not expect to see the same phenotype with the N-terminal domain since an earlier report for class IIb LysRS indicated that the N-terminal anticodon-binding domain was not able to aminoacylate tRNA^{Lys} [48]. Nonetheless, the overexpression of the anticodon binding domain of *H. pylori* ND-AspRS is toxic to *E. coli* host cells (Fig. 2). Therefore, the overexpression time was limited to 30 min in order to minimize toxicity. The protein was purified to greater than 95% homogeneity by SDS–PAGE as reported [24] with a slight modification (See material and methods) and confirmed by Western blotting (Fig. 3). The purified protein was obtained in good yield of 6.9 mg per 1 L culture despite the short overexpression time. Although lower yield is expected when LB medium is replaced by minimal media for isotopically labeled protein preparation, this can simply be overcome by utilizing larger cell culture. The optimization for isotopically labeled protein preparation is in progress.

For biophysical characterization and crystallization, the protein was further purified using gel filtration chromatography. The protein was determined to be monomeric, with an average molecular

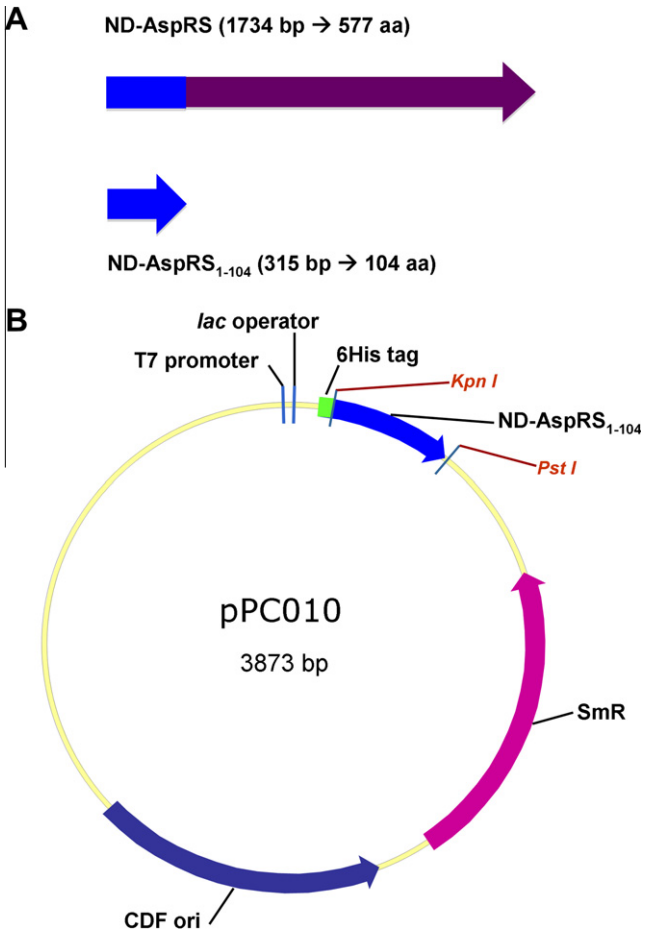

Fig. 1. Cloning of the ND-AspRS$_{1\text{-}104}$ from *H. pylori*. (A) Schematic representation of the wild-type and the ND-AspRS$_{1\text{-}104}$ genes from *H. pylori*. (B) Schematic representation of pPC010, a pCDF-1b-derived expression vector producing the ND-AspRS$_{1\text{-}104}$ with 6 histidine affinity tag at the N-terminus.

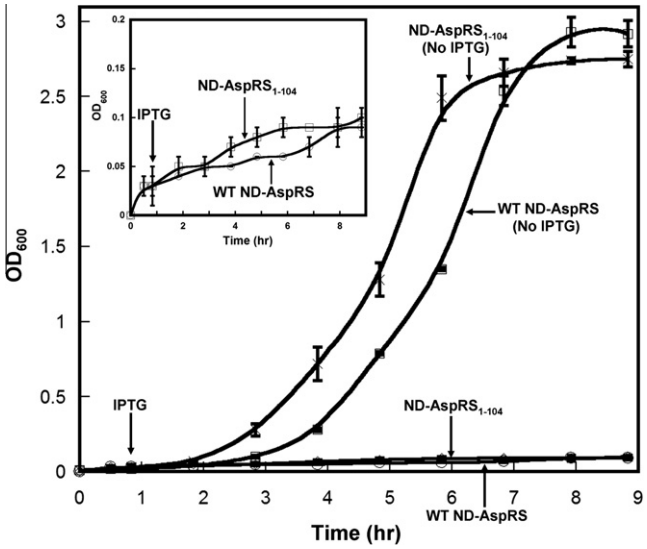

Fig. 2. Heterologous overexpression of the ND-AspRS$_{1-104}$ from *H. pylori* in *E. coli* BL21(DE3) host cells. Overexpression of the ND-AspRS$_{1-104}$ is toxic to *E. coli* host cells compared with cultures without protein expression (No IPTG). The same phenotype is observed when wild-type ND-AspRS from *H. pylori* is overexpressed in similar host cells (shown in the inset).

weight of 15.5 kDa compared to the calculated monomeric mass of 12.87 kDa (Fig. 4). Although class IIb aminoacyl-tRNA synthetases, such as ND-AspRS, exist in a solution as homodimers [49], dimerization requires direct contacts between the anticodon-binding domain of one monomer to the catalytic domain of the other monomer. In the absence of the catalytic domain, the ND-AspRS$_{1-104}$ is monomeric, in agreement with studies of the class IIb N-terminal anticodon-binding domain of *Bacillus stearothermophilus* LysRS [48].

Growth studies

It is well documented that heterologous overexpression of ND-AspRS [24], ND-GluRS [16,50,51], or GluRS2 [21] in *E. coli* host cells results in toxic phenotype. The toxicity was proven to originate from generation of incorrectly aminoacylated tRNA (Glu-tRNA^{Gln} in the case of ND-GluRS and GluRS2, Asp-tRNA^{Asn} in the case of ND-AspRS). However, the toxicity can be partially rescued by co-expression of GatCAB from *H. pylori* with ND-AspRS [24]. Since the N-terminal anticodon-binding domain of *B. stearothermophilus* lacks the ability to aminoacylate tRNA^{Lys} [48], we anticipated that the ND-AspRS$_{1-104}$ of *H. pylori* would lack the ability to generate incorrectly aminoacylated Asp-tRNA^{Asn}, the causal species for toxicity.

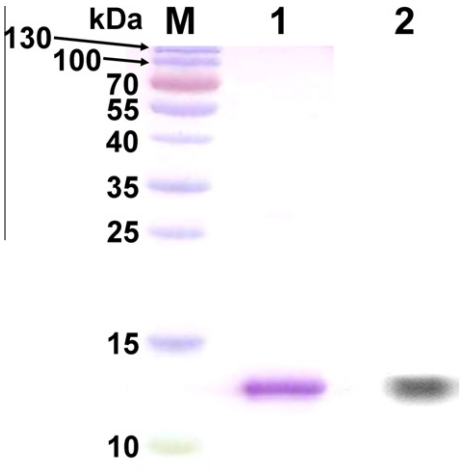

Fig. 3. SDS–PAGE and Western blot analysis of the purified ND-AspRS$_{1-104}$ from *H. pylori*. The electrophoresis was conducted on 8% separating gel with Coomassie brilliant blue staining. Lane M, protein markers; lane 1, purified ND-AspRS$_{1-104}$; lane 2, Western blot of the ND-AspRS$_{1-104}$.

Overexpression of the *H. pylori* ND-AspRS$_{1-104}$ was, however, toxic to *E. coli* (Fig. 2). Generally, the anticodon-binding domain of AspRSs contains an OB (oligonucleotide/oligosaccharide binding) fold, which contains five β-strands forming a closed β-barrel with an α-helix connecting the third and the fourth strand [52], and the toxicity may arise from the interaction between the ND-AspRS$_{1-104}$ and nucleotides, presumably tRNA^{Asp} and/or tRNA^{Asn}, in the host cells, causing depletion of tRNAs available to protein biosynthesis. High level of the *H. pylori* ND-AspRS$_{1-104}$ in the host cells may also disrupt the dimerization of the native *E. coli* AspRS, compromising the aspartylation activity of the enzyme. The precise molecular mechanism contributing to the observed toxicity has, however, yet to be determined experimentally.

Dynamic light scattering reveals thermal stability of the H. pylori ND-AspRS$_{1-104}$

To assess the thermal stability and melting point of the *H. pylori* ND-AspRS$_{1-104}$, we used DLS to follow the monodispersity of the protein in solution as a function of temperature [53]. This method has been used previously to monitor aggregation of asparaginyl-, valyl-, and leucyl-tRNA synthetases from *E. coli* [54]. The ND-AspRS$_{1-104}$ showed uniform particle size over a temperature range of 20–42 °C, and an exponential increase in particle size at >42 °C that was indicative of protein denaturation (Fig. 5). The expanded plot in Fig. 5 indicates that at lower temperatures, the average particle size was 10 nm and in line with the average particle diameter reported for the wild-type AspRS from *Plasmodium falciparum* (11.7 nm) [55]. The results from our measurement implied the existence of a stable, geometrically well-defined protein at the temperature below 42 °C.

Circular dichroism spectroscopy reveals changes in secondary structure content at high temperature

The CD spectrum recorded at 20 °C (Fig. 6) showed a mixture of β-sheet (36.7%) (minimum around 214 nm) and α-helix (38.7%) (minima around 209 and 222 nm) [56,57] although crystal structures of *E. coli* AspRS indicated approximately 48% β-sheet and 21% α-helix in the ND-AspRS$_{1-104}$ [58,59]. This deviation may be due to insufficient data representation in the basis set used in secondary structure calculation or differences in the anticodon-binding domain of *H. pylori* ND-AspRS. The secondary structure content of the protein remained relatively constant up to 60 °C followed by a transition from α-helix to β-sheet between 60 and 70 °C. Subsequent cooling of the sample showed that this thermal transition was irreversible. The changes detected by CD occurred at higher temperature than the melting temperature determined by DLS suggesting that the protein may undergo tertiary structural changes with very small alteration in secondary structure content at lower temperature that leads to aggregation but presumably with minimal change in secondary structure content. From the DLS and CD spectroscopic data, it was apparent, however, that the ND-AspRS$_{1-104}$ of *H. pylori* was stable at physiological condition and suitable for NMR spectroscopic measurements and crystallization trials.

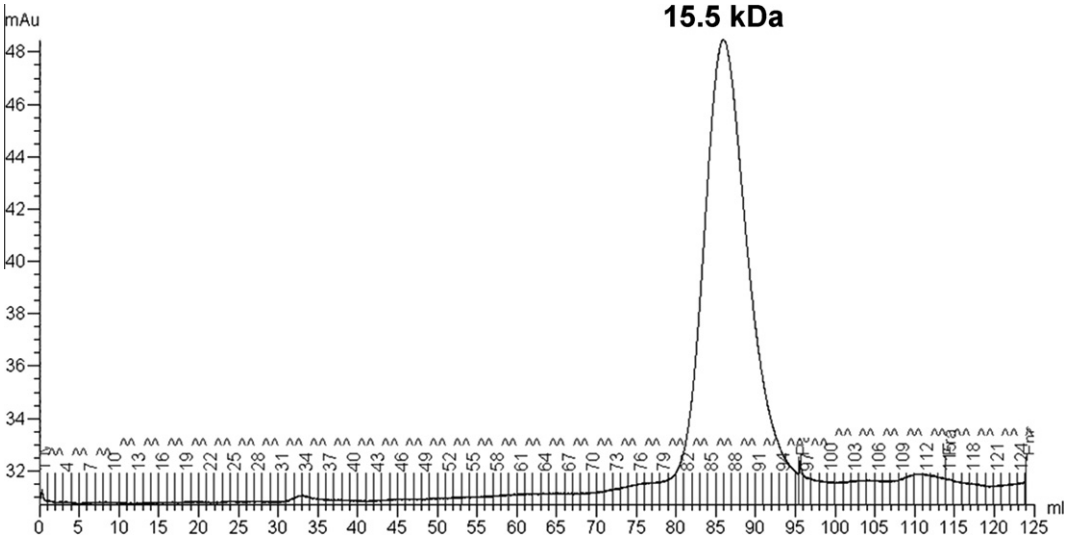

Fig. 4. Gel filtration chromatogram of the ND-AspRS$_{1-104}$. The protein eluted between 80 and 95 mL with the center of the peak at 86 mL. The molecular weight was calculated to be 15.5 kDa, in agreement with isotopically average molecular weight (12,870.9 Da) for the monomeric state of this protein.

1D ^{1}H NMR spectroscopy and X-ray crystallography

The ND-AspRS$_{1-104}$ was initially subjected to a series of solubility tests at various pH, buffer concentrations, and protein concentrations. The optimal conditions were 250 μM protein, 50 mM phosphate buffer, 150 mM sodium chloride at pH 8.0; under these conditions, the protein remained stable over 10 days. Acquisition of 1D ^{1}H NMR data in this buffer showed good dispersion of the NMR signals indicative of folded protein and significant β-sheet content (signals around 5–6 ppm in Fig. 7).

The protein was then subjected to crystal screening as initial crystallization using a microbatch tray. The drops showed crystallization in the first few days of incubation and were regularly checked for 3 months. Among all screened conditions, the major precipitant PEG 4000 gave the best crystal formation. Our truncated version of the ND-AspRS from *H. pylori* formed crystals at pH 5.6 with 30% (w/v) PEG 4000, 100 mM ammonium sulfate, 100 mM sodium citrate after 2 days (Fig. 8A). The absence of crystal formation in a no-protein control plate (Fig. 8B) clearly confirmed the formation of protein crystals. These acidic crystallization conditions distinguish this domain from the conditions used to crystallize full-length AspRS enzymes (e.g. pH 7.25 for *Entamoeba histolytica* AspRS [60], pH 6.8 for *E. coli* AspRS [59], pH 7.5 for *Thermus thermophilus* AspRS [61]), and the highly basic (pH 9.5) for AspRS-2 from *T. thermophilus* crystallization [62]). Further optimization of these initial crystallization conditions is currently in progress to obtain diffraction quality crystals.

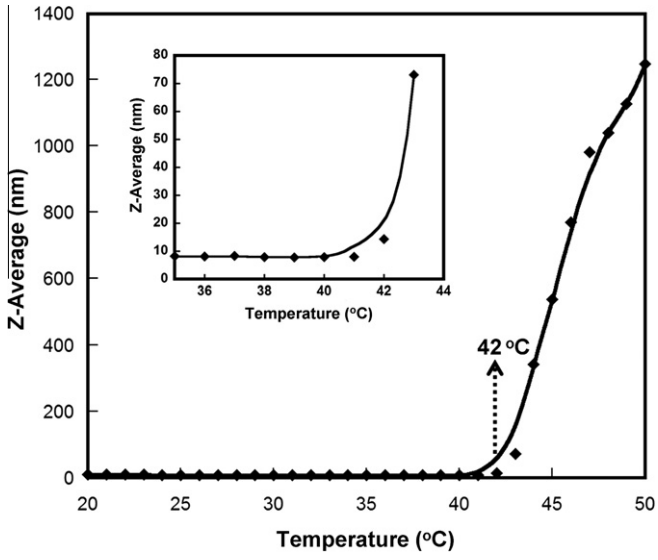

Fig. 5. Dynamic light scattering analysis of the ND-AspRS$_{1-104}$. The protein was subjected to the temperature-dependent DLS measurements. The average particle size, described as Z-average diameter, at low temperature is approximately 10 nm (shown in the inset). Denatured aggregates were detected at >42 °C.

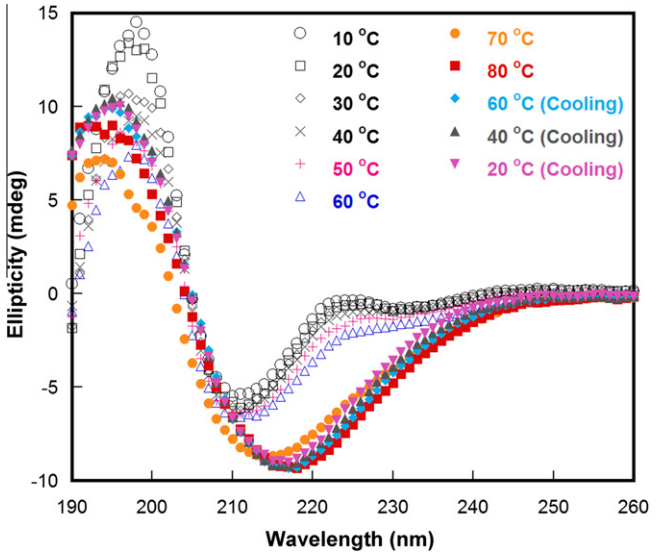

Fig. 6. Circular dichroism (CD) spectra of the ND-AspRS$_{1-104}$. Spectra were recorded over a range of 190–260 nm, and 10–80 °C with 10 °C interval. The sample was then cooled down, and the spectra were rerecorded every 20 °C. The CD spectra indicated a mixture of β-sheet (minimum around 214 nm) and α-helix (minima around 209 and 222 nm) at low temperature (10–40 °C). Transition from a mixed β-sheet α-helix state to primarily β-sheet was evidenced from 60 to 70 °C. All spectra from cooling entries indicated that the observed secondary structure transitions were irreversible.

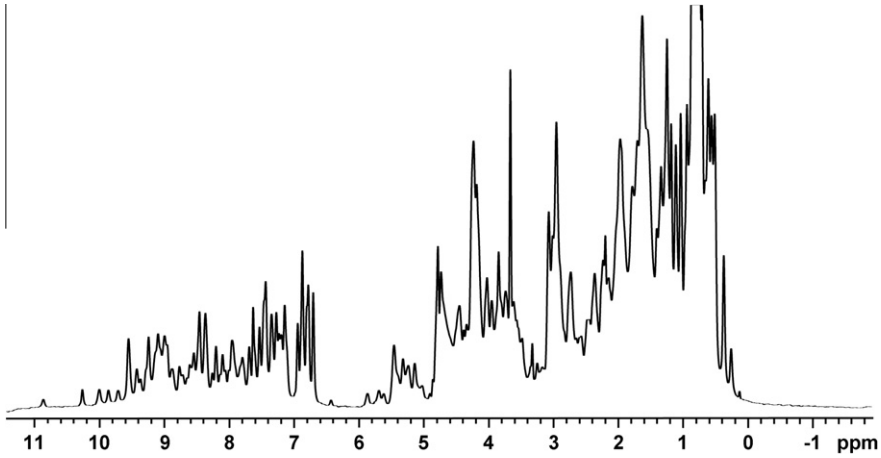

Fig. 7. The 1D ^{1}H NMR spectrum of the ND-AspRS$_{1-104}$. The protein was subjected to a standard 1D DPFGSE experiment at 25 °C on a 600 MHz Varian VNMRS cryo-probe equipped spectrometer. The spectrum demonstrated good NMR signal dispersion; an indication of folded protein, with significant β-sheet content (signals around 5–6 ppm).

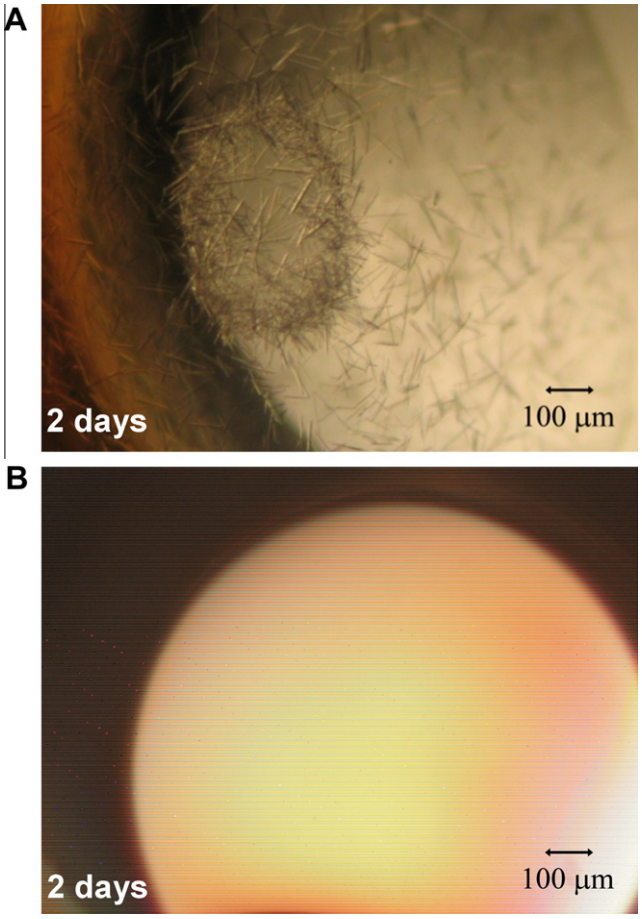

Fig. 8. Crystallization of the ND-AspRS$_{1-104}$. (A) Crystal formation after 2 days in a microbatch tray containing 30% (w/v) PEG 4000, 100 mM ammonium sulfate, 100 mM sodium citrate at pH 5.6. (B) No-protein control experiment in a microbatch tray under identical crystallization condition confirmed the formation of protein crystals. The incubation temperature was 18 °C for all experiments.

Conclusions

We have reported the cloning, over-expression, and purification of the ND-AspRS$_{1-104}$ from the human pathogen *H. pylori*. Intriguingly, overexpression of this protein in *E. coli* host cells resulted in a toxic phenotype which was also observed for the heterologous overexpression of the full length wild-type enzyme [24]. The stability of the protein was evidenced by temperature-dependent dynamic light scattering experiments where the protein melted at 42 °C. Unlike the full length AspRS enzyme, which is a homodimer in solution [49], the ND-AspRS$_{1-104}$ is monomeric when analyzed by gel filtration chromatography. The protein is folded according to 1D ^{1}H NMR and CD spectra. The temperature-dependent CD spectra indicated a transition from a mixed β-sheet/α-helix state to predominantly β-sheet between 60 and 70 °C. These tightly packed β-sheets appeared to be very stable and maintained their secondary structure integrity even when the temperature was decreased to 20 °C. Finally, successful crystallization trials were obtained from conditions containing PEG 4000 as the major precipitant. This work provides the basis for future NMR and X-ray crystallography studies aimed at understanding the dual tRNA specificity arising from the interaction between the anticodon-binding domain and its tRNA isoacceptors.

Acknowledgments

This work was supported by the Kasetsart University Research and Development Institute (KURDI), and the faculty of science, Kasetsart University under the pre-proposal research fund (PRF4/2550), and science research fund (ScRF-E3/2551 and ScRF-E4/2552). We thank Professor Chartchai Krittanai (Institute of Molecular Biosciences, Mahidol University, Nakhonpathom, Thailand), and Professor Catherine Florentz (Université de Strasbourg, IBMC, France) for informative discussion regarding CD and DLS experiments. We thank Ms.Ruethaitip Tiratrakulvichaya (DKSH (Thailand) Limited), Professor Kiattawee Choowongkomon, and Professor Nonlawat Boonyalai (Department of Biochemistry, Kasetsart University), for access to their research instruments, and the EPSRC for the Bristol NMR facility (EP/F013515). Financial support from the Center of Excellence for Innovation in Chemistry (PERCH-CIC), Commission on Higher Education, Ministry of Education is also gratefully acknowledged.

References

[1] M. Ibba, D. Soll, Aminoacyl-tRNAs: setting the limits of the genetic code, Genes. Dev. 18 (2004) 731–738.
[2] M. Ibba, D. Soll, Aminoacyl-tRNA synthesis, Annu. Rev. Biochem. 69 (2000) 617–650.
[3] L.R. de Pouplana, P. Schimmel, A view into the origin of life: aminoacyl-tRNA synthetases, Cell. Mol. Life Sci. 57 (2000) 865–870.
[4] T. Cathopoulis, P. Chuawong, T.L. Hendrickson, Novel tRNA aminoacylation mechanisms, Mol. Biosyst. 3 (2007) 408–418.

[5] P. O'Donoghue, K. Sheppard, O. Nureki, D. Soll, Rational design of an evolutionary precursor of glutaminyl-tRNA synthetase, Proc. Natl. Acad. Sci. USA 108 (2011) 20485–20490.

[6] T. Rampias, K. Sheppard, D. Soll, The archaeal transamidosome for RNA-dependent glutamine biosynthesis, Nucleic Acids Res. 38 (2010) 5774–5783.

[7] S. Paravisi, G. Fumagalli, M. Riva, P. Morandi, R. Morosi, P.V. Konarev, M.V. Petoukhov, S. Bernier, R. Chenevert, D.I. Svergun, B. Curti, M.A. Vanoni, Kinetic and mechanistic characterization of *Mycobacterium tuberculosis* glutamyl-tRNA synthetase and determination of its oligomeric structure in solution, FEBS J. 276 (2009) 1398–1417.

[8] M. Frechin, A.M. Duchene, H.D. Becker, Translating organellar glutamine codons: a case by case scenario?, RNA biol 6 (2009) 31–34.

[9] C. Pujol, M. Bailly, D. Kern, L. Marechal-Drouard, H. Becker, A.M. Duchene, Dual-targeted tRNA-dependent amidotransferase ensures both mitochondrial and chloroplastic Gln-tRNA^{Gln} synthesis in plants, Proc. Natl. Acad. Sci. USA 105 (2008) 6481–6485.

[10] H. Nunez, C. Lefimil, B. Min, D. Soll, O. Orellana, In vivo formation of glutamyl-tRNA(Gln) in *Escherichia coli* by heterologous glutamyl-tRNA synthetases, FEBS Lett. 557 (2004) 133–135.

[11] J.C. Salazar, I. Ahel, O. Orellana, D. Tumbula-Hansen, R. Krieger, L. Daniels, D. Soll, Coevolution of an aminoacyl-tRNA synthetase with its tRNA substrates, Proc. Natl. Acad. Sci. USA 100 (2003) 13863–13868.

[12] A.W. Curnow, D.L. Tumbula, J.T. Pelaschier, B. Min, D. Soll, Glutamyl-tRNA(Gln) amidotransferase in *Deinococcus radiodurans* may be confined to asparagine biosynthesis, Proc. Natl. Acad. Sci. USA 95 (1998) 12838–12843.

[13] G. Raczniak, H.D. Becker, B. Min, D. Soll, A single amidotransferase forms asparaginyl-tRNA and glutaminyl-tRNA in *Chlamydia trachomatis*, J. Biol. Chem. 276 (2001) 45862–45867.

[14] A. Schon, C.G. Kannangara, S. Gough, D. Soll, Protein biosynthesis in organelles requires misaminoacylation of tRNA, Nature 331 (1988) 187–190.

[15] M. Wilcox, M. Nirenberg, Transfer RNA as a cofactor coupling amino acid synthesis with that of protein, Proc. Natl. Acad. Sci. USA 61 (1968) 229–236.

[16] J. Lapointe, L. Duplain, M. Proulx, A single glutamyl-tRNA synthetase aminoacylates tRNA^{Glu} and tRNA^{Gln} in *Bacillus subtilis* and efficiently misacylates *Escherichia coli* tRNA^{Gln1} in vitro, J. Bacteriol. 165 (1986) 88–93.

[17] L.T. Guo, S. Helgadottir, D. Soll, J. Ling, Rational design and directed evolution of a bacterial-type glutaminyl-tRNA synthetase precursor, Nucleic Acids Res. 40 (2012) 7967–7974.

[18] J.L. Huot, F. Fischer, J. Corbeil, E. Madore, B. Lorber, G. Diss, T.L. Hendrickson, D. Kern, J. Lapointe, Gln-tRNA^{Gln} synthesis in a dynamic transamidosome from *Helicobacter pylori*, where GluRS2 hydrolyzes excess Glu-tRNA^{Gln}, Nucleic Acids Res. 39 (2011) 9306–9315.

[19] K.M. Chang, T.L. Hendrickson, Recognition of tRNA^{Gln} by *Helicobacter pylori* GluRS2–a tRNA^{Gln}-specific glutamyl-tRNA synthetase, Nucleic Acids Res. 37 (2009) 6942–6949.

[20] J. Lee, T.L. Hendrickson, Divergent anticodon recognition in contrasting glutamyl-tRNA synthetases, J. Mol. Biol. 344 (2004) 1167–1174.

[21] S. Skouloubris, L. Ribas de Pouplana, H. De Reuse, T.L. Hendrickson, A noncognate aminoacyl-tRNA synthetase that may resolve a missing link in protein evolution, Proc. Natl. Acad. Sci. USA 100 (2003) 11297–11302.

[22] F. Fischer, J.L. Huot, B. Lorber, G. Diss, T.L. Hendrickson, H.D. Becker, J. Lapointe, D. Kern, The asparagine-transamidosome from *Helicobacter pylori*: a dual-kinetic mode in non-discriminating aspartyl-tRNA synthetase safeguards the genetic code, Nucleic Acids Res. 40 (2012) 4965–4976.

[23] A.M. Cardoso, C. Polycarpo, O.B. Martins, D. Soll, A non-discriminating aspartyl-tRNA synthetase from *Halobacterium salinarum*, RNA Biol. 3 (2006) 110–114.

[24] P. Chuawong, T.L. Hendrickson, The nondiscriminating aspartyl-tRNA synthetase from *Helicobacter pylori*: anticodon-binding domain mutations that impact tRNA specificity and heterologous toxicity, Biochemistry 45 (2006) 8079–8087.

[25] D. Bernard, P.M. Akochy, D. Beaulieu, J. Lapointe, P.H. Roy, Two residues in the anticodon recognition domain of the aspartyl-tRNA synthetase from *Pseudomonas aeruginosa* are individually implicated in the recognition of tRNA^{Asn}, J. Bacteriol. 188 (2006) 269–274.

[26] L. Feng, J. Yuan, H. Toogood, D. Tumbula-Hansen, D. Soll, Aspartyl-tRNA synthetase requires a conserved proline in the anticodon-binding loop for tRNA(Asn) recognition in vivo, J. Biol. Chem. 280 (2005) 20638–20641.

[27] P.M. Akochy, D. Bernard, P.H. Roy, J. Lapointe, Direct glutaminyl-tRNA biosynthesis and indirect asparaginyl-tRNA biosynthesis in *Pseudomonas aeruginosa* PAO1, J. Bacteriol. 186 (2004) 767–776.

[28] B. Min, M. Kitabatake, C. Polycarpo, J. Pelaschier, G. Raczniak, B. Ruan, H. Kobayashi, S. Namgoong, D. Soll, Protein synthesis in *Escherichia coli* with mischarged tRNA, J. Bacteriol. 185 (2003) 3524–3526.

[29] L. Feng, D. Tumbula-Hansen, H. Toogood, D. Soll, Expanding tRNA recognition of a tRNA synthetase by a single amino acid change, Proc. Natl. Acad. Sci. USA 100 (2003) 5676–5681.

[30] C. Charron, H. Roy, M. Blaise, R. Giege, D. Kern, Non-discriminating and discriminating aspartyl-tRNA synthetases differ in the anticodon-binding domain, EMBO J. 22 (2003) 1632–1643.

[31] D. Tumbula-Hansen, L. Feng, H. Toogood, K.O. Stetter, D. Soll, Evolutionary divergence of the archaeal aspartyl-tRNA synthetases into discriminating and nondiscriminating forms, J. Biol. Chem. 277 (2002) 37184–37190.

[32] H.D. Becker, H. Roy, L. Moulinier, M.H. Mazauric, G. Keith, D. Kern, *Thermus thermophilus* contains an eubacterial and an archaebacterial aspartyl-tRNA synthetase, Biochemistry 39 (2000) 3216–3230.

[33] H.D. Becker, D. Kern, *Thermus thermophilus*: a link in evolution of the tRNA-dependent amino acid amidation pathways, Proc. Natl. Acad. Sci. USA 95 (1998) 12832–12837.

[34] H.D. Becker, J. Reinbolt, R. Kreutzer, R. Giege, D. Kern, Existence of two distinct aspartyl-tRNA synthetases in *Thermus thermophilus*. Structural and biochemical properties of the two enzymes, Biochemistry 36 (1997) 8785–8797.

[35] F. Charriere, P. O'Donoghue, S. Helgadottir, L. Marechal-Drouard, M. Cristodero, E.K. Horn, D. Soll, A. Schneider, Dual targeting of a tRNA^{Asp} requires two different aspartyl-tRNA synthetases in *Trypanosoma brucei*, J. Biol. Chem. 284 (2009) 16210–16217.

[36] J.C. Salazar, R. Zuniga, G. Raczniak, H. Becker, D. Soll, O. Orellana, A dual-specific Glu-tRNA(Gln) and Asp-tRNA(Asn) amidotransferase is involved in decoding glutamine and asparagine codons in *Acidithiobacillus ferrooxidans*, FEBS Lett. 500 (2001) 129–131.

[37] H.D. Becker, B. Min, C. Jacobi, G. Raczniak, J. Pelaschier, H. Roy, S. Klein, D. Kern, D. Soll, The heterotrimeric *Thermus thermophilus* Asp-tRNA(Asn) amidotransferase can also generate Gln-tRNA(Gln), FEBS Lett. 476 (2000) 140–144.

[38] A.W. Curnow, K. Hong, R. Yuan, S. Kim, O. Martins, W. Winkler, T.M. Henkin, D. Soll, Glu-tRNA^{Gln} amidotransferase: a novel heterotrimeric enzyme required for correct decoding of glutamine codons during translation, Proc. Natl. Acad. Sci. USA 94 (1997) 11819–11826.

[39] F.R. Blattner, G. Plunkett 3rd, C.A. Bloch, N.T. Perna, V. Burland, M. Riley, J. Collado-Vides, J.D. Glasner, C.K. Rode, G.F. Mayhew, J. Gregor, N.W. Davis, H.A. Kirkpatrick, M.A. Goeden, D.J. Rose, B. Mau, Y. Shao, The complete genome sequence of *Escherichia coli* K-12, Science 277 (1997) 1453–1474.

[40] K. Sheppard, P.M. Akochy, J.C. Salazar, D. Soll, The *Helicobacter pylori* amidotransferase GatCAB is equally efficient in glutamine-dependent transamidation of Asp-tRNA^{Asn} and Glu-tRNA^{Gln}, J. Biol. Chem. 282 (2007) 11866–11873.

[41] J.L. Huot, C. Balg, D. Jahn, J. Moser, A. Emond, S.P. Blais, R. Chenevert, J. Lapointe, Mechanism of a GatCAB amidotransferase: aspartyl-tRNA synthetase increases its affinity for Asp-tRNA(Asn) and novel aminoacyl-tRNA analogues are competitive inhibitors, Biochemistry 46 (2007) 13190–13198.

[42] Y. Sato, Y. Maeda, S. Shimizu, M.T. Hossain, S. Ubukata, K. Suzuki, T. Sekiguchi, A. Takenaka, Structure of the nondiscriminating aspartyl-tRNA synthetase from the crenarchaeon *Sulfolobus tokodaii* strain 7 reveals the recognition mechanism for two different tRNA anticodons, Acta Crystallogr. D Biol. Crystallogr. 63 (2007) 1042–1047.

[43] E. Schmitt, L. Moulinier, S. Fujiwara, T. Imanaka, J.C. Thierry, D. Moras, Crystal structure of aspartyl-tRNA synthetase from *Pyrococcus kodakaraensis* KOD: archaeon specificity and catalytic mechanism of adenylate formation, EMBO J. 17 (1998) 5227–5237.

[44] M. Blaise, M. Bailly, M. Frechin, M.A. Behrens, F. Fischer, C.L. Oliveira, H.D. Becker, J.S. Pedersen, S. Thirup, D. Kern, Crystal structure of a transfer-ribonucleoprotein particle that promotes asparagine formation, EMBO J. 29 (2010) 3118–3129.

[45] N. Sreerama, R.W. Woody, Estimation of protein secondary structure from circular dichroism spectra: comparison of CONTIN, SELCON, and CDSSTR methods with an expanded reference set, Anal. Biochem. 287 (2000) 252–260.

[46] K. Stott, J. Stonehouse, J. Keeler, T.-L. Hwang, A.J. Shaka, Excitation sculpting in high-resolution nuclear magnetic resonance spectroscopy: application to selective NOE experiments, J. Am. Chem. Soc. 117 (1995) 4199–4200.

[47] C. Combet, M. Jambon, G. Deleage, C. Geourjon, Geno3D: automatic comparative molecular modelling of protein, Bioinformatics 18 (2002) 213–214.

[48] T. Takita, K. Inouye, Transition state stabilization by the N-terminal anticodon-binding domain of lysyl-tRNA synthetase, J. Biol. Chem. 277 (2002) 29275–29282.

[49] R. Giegé, B. Rees, Aspartyl-tRNA synthetases, in: M. Ibba, C. Francklyn, S. Cusak (Eds.), The Aminoacyl-tRNA Synthetases, Landes Bioscience, Texas, 2005, pp. 210–226.

[50] J.W. Baick, J.H. Yoon, S. Namgoong, D. Soll, S.I. Kim, S.H. Eom, K.W. Hong, Growth inhibition of *Escherichia coli* during heterologous expression of *Bacillus subtilis* glutamyl-tRNA synthetase that catalyzes the formation of mischarged glutamyl-tRNA1 Gln, J. Microbiol. 42 (2004) 111–116.

[51] M. Pelchat, L. Lacoste, F. Yang, J. Lapointe, Overproduction of the *Bacillus subtilis* glutamyl-tRNA synthetase in its host and its toxicity to *Escherichia coli*, Can. J. Microbiol. 44 (1998) 378–381.

[52] A.G. Murzin, OB(oligonucleotide/oligosaccharide binding)-fold: common structural and functional solution for non-homologous sequences, EMBO J. 12 (1993) 861–867.

[53] N. Chayen, M. Dieckmann, K. Dierks, P. Fromme, Size and shape determination of proteins in solution by a noninvasive depolarized dynamic light scattering instrument, Ann. NY Acad. Sci. 1027 (2004) 20–27.

[54] F. Thibault, J. Langowski, R. Leberman, Pre-nucleation crystallization studies on aminoacyl-tRNA synthetases by dynamic light-scattering, J. Mol. Biol. 225 (1992) 185–191.

[55] T. Bour, A. Akaddar, B. Lorber, S. Blais, C. Balg, E. Candolfi, M. Frugier, Plasmodial aspartyl-tRNA synthetases and peculiarities in *Plasmodium falciparum*, J. Biol. Chem. 284 (2009) 18893–18903.

[56] S.M. Kelly, N.C. Price, The use of circular dichroism in the investigation of protein structure and function, Curr. Protein Pept. Sci. 1 (2000) 349–384.

[57] W.C. Johnson Jr., Protein secondary structure and circular dichroism: a practical guide, Proteins 7 (1990) 205–214.

[58] L. Moulinier, S. Eiler, G. Eriani, J. Gangloff, J.C. Thierry, K. Gabriel, W.H. McClain, D. Moras, The structure of an AspRS-tRNA(Asp) complex reveals a tRNA-dependent control mechanism, EMBO J. 20 (2001) 5290–5301.
[59] S. Eiler, A. Dock-Bregeon, L. Moulinier, J.C. Thierry, D. Moras, Synthesis of aspartyl-tRNA(Asp) in *Escherichia coli* – a snapshot of the second step, EMBO J. 18 (1999) 6532–6541.
[60] E.A. Merritt, T.L. Arakaki, E.T. Larson, A. Kelley, N. Mueller, A.J. Napuli, L. Zhang, G. Deditta, J. Luft, C.L. Verlinde, E. Fan, F. Zucker, F.S. Buckner, W.C. Van Voorhis, W.G. Hol, Crystal structure of the aspartyl-tRNA synthetase from *Entamoeba histolytica*, Mol. Biochem. Parasitol. 169 (2010) 95–100.
[61] C. Briand, A. Poterszman, S. Eiler, G. Webster, J. Thierry, D. Moras, An intermediate step in the recognition of tRNA(Asp) by aspartyl-tRNA synthetase, J. Mol. Biol. 299 (2000) 1051–1060.
[62] C. Charron, H. Roy, B. Lorber, D. Kern, R. Giege, Crystallization and preliminary X-ray diffraction data of the second and archaebacterial-type aspartyl-tRNA synthetase from *Thermus thermophilus*, Acta Crystallogr. D Biol. Crystallogr. 57 (2001) 1177–1179.